

1 Contribution of particle-induced lysosomal membrane hyperpolarization to lysosomal
2 membrane permeabilization

3 Tahereh Ziglari¹, Zifan Wang², Andrij Holian^{1*}

4 **Supplementary data**

5

Table S1. Physiochemical characteristics of ENM and SiO₂.

Quality	Technique	ZnO NP	TiO ₂	CeO ₂	SiO ₂
Size (nm)	TEM	~30	~25	~25	500-1000
Size in RPMI media (nm ±SD)	DLS	215±15	1025±137	1154±140	1029±165
Zeta potential in H ₂ O at pH 6 (mV±SD)	Zetasizer	-28.2±0.5	17.3±0.9	24.8±0.49	-46±1.48

6

7 **Table S1.** Physiochemical characteristics of three NP and SiO₂. Average particle
8 size was assessed using ImageJ software. DLS measurement was based on intensity.

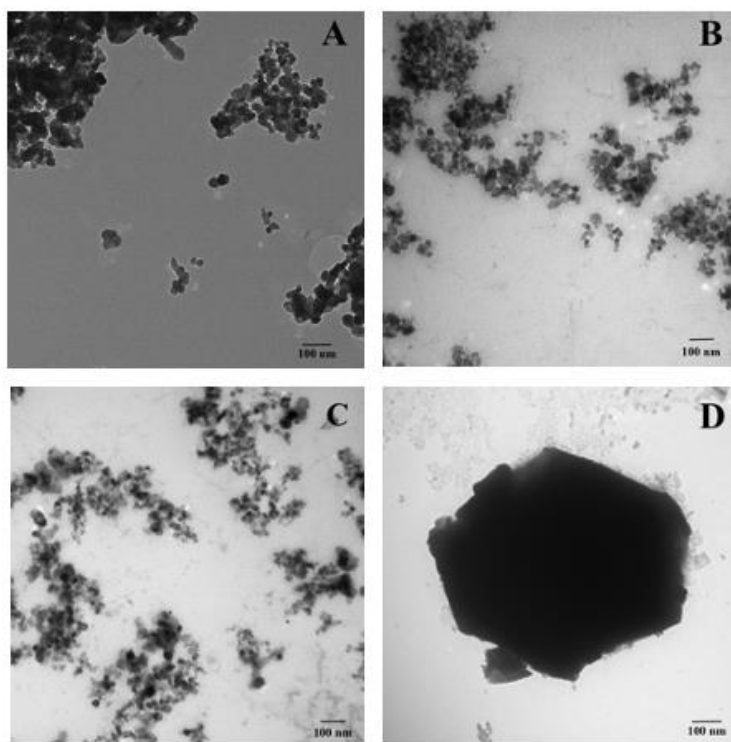
Table S2. Lysosomal membrane potential calculation using Nernst equation.

	Cc/CL ratio of ~100 cells per group	Lysosomal membrane potential ($\psi\phi$)= RT/zF ln Cc/CL
Control	58.27/142.89 = 0.4	0.023 J/C = 0.023 V= 23 mV
ZnO	60.43/600.12= 0.1	0.06 J/C = 0.06 V= 60 mV
TiO ₂	62.76/223.45= 0.223	0.04 J/C = 0.04 V= 40 mV
CeO ₂	54.32/234.78= 0.23	0.038 J/C = 0.038 V= 38 mV
SiO ₂	56.24/466.66= 0.12	0.055 J/C = 0.055 V= 55 mV

9

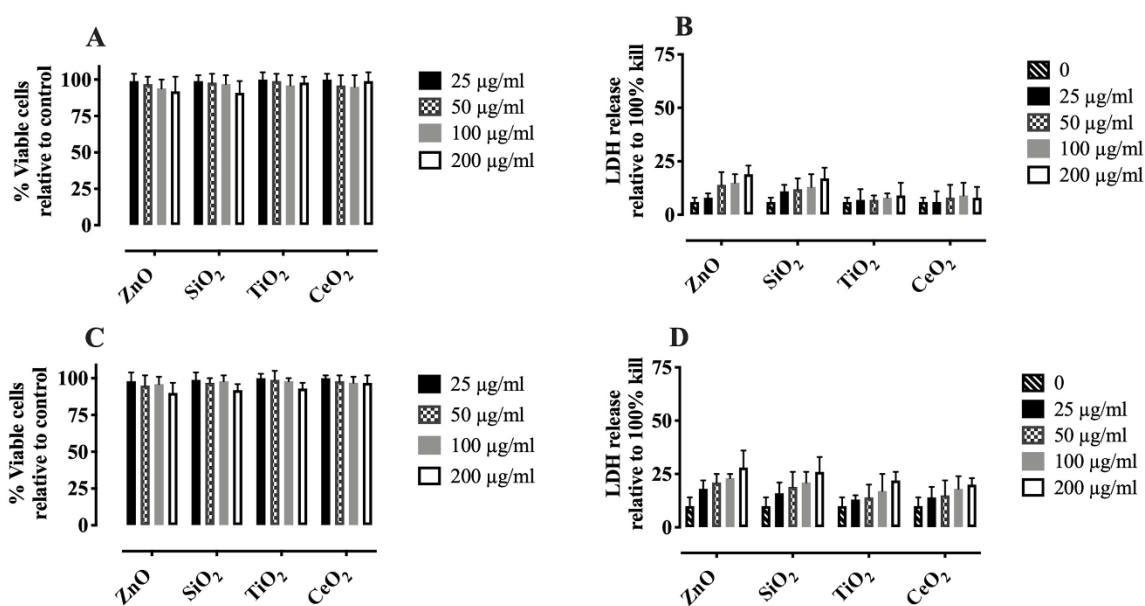
10

11 **Table S2.** Lysosomal membrane potential calculation using Nernst equation. AM were
 12 incubated with individual NP or SiO₂ for 1 hr at 37°C. C_C/C_L ratio was measured in 100
 13 cells per each group and lysosomal membrane potential was calculated as discussed in
 14 the Methods.



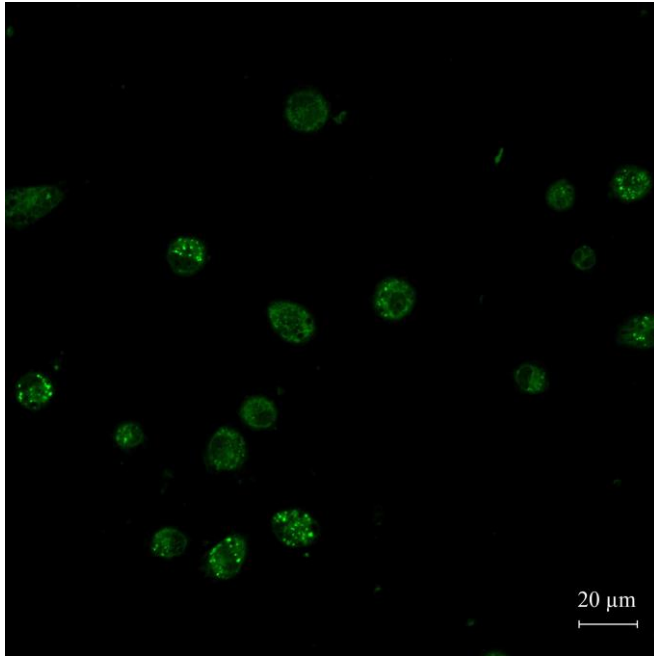
15

16 **Figure S1.** Transmission electron microscopy images of NP and SiO₂ in PBS
 17 buffer. A) ZnO, B) TiO₂, C) CeO₂, and D) SiO₂ are shown. An average particle size
 18 was assessed using ImageJ software.



19

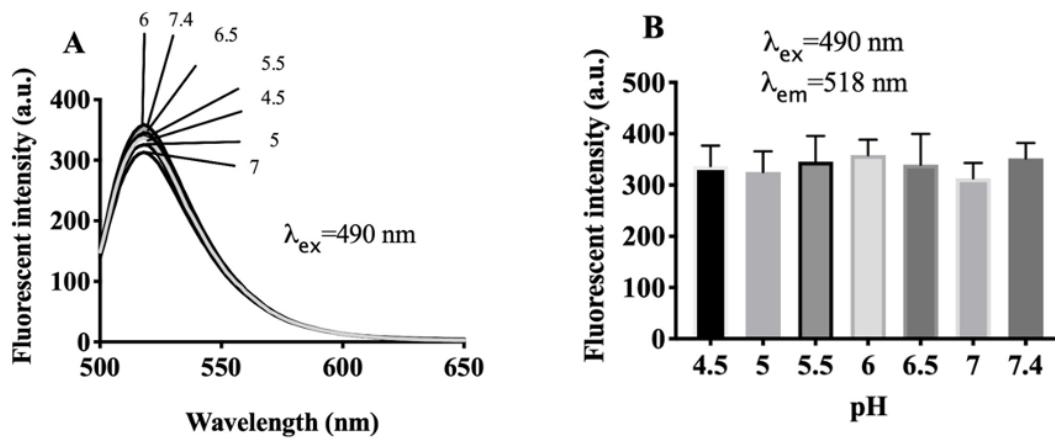
20 **Figure S2. Time-course toxicity in AM attributable to NP and SiO₂.** AM were
21 incubated with individual particles for 1 and 2 hr at 37°C. Results from the **A)** MTS
22 assay after incubation of particles with AM for 1 hr, **B)** LDH assay after incubation of
23 particles with AM for 1 hr, **C)** MTS assay after incubation of particles with AM for 2 hr
24 **D)** LDH assay after incubation of particles with AM for 1 hr. Data are presented as
25 means \pm SE of triplicate measurements.



26

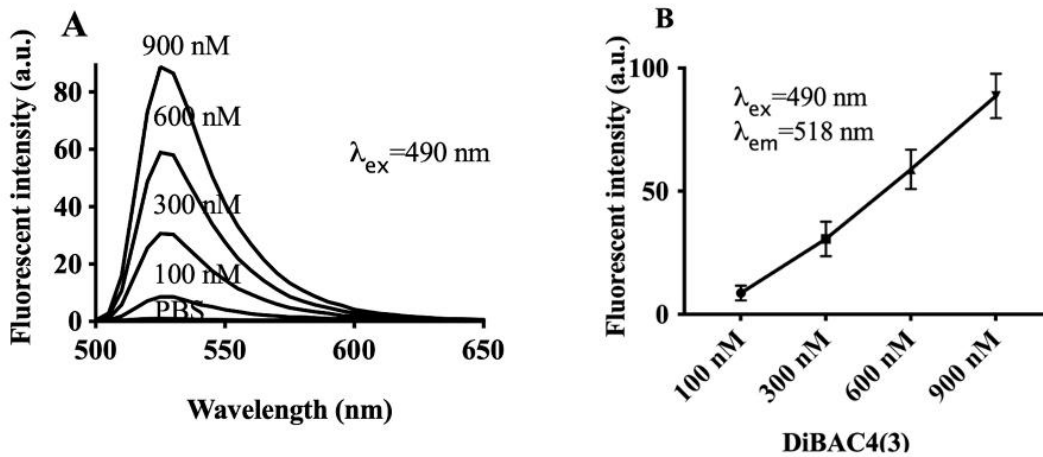
27 **Figure S3. Accumulation of DiBAC4(3) in the lysosomes of AM.** AM were
28 incubated with 300 nm DiBAC4(3) for 10 min in PBS at 37°C. A Zeiss LSM 880
29 confocal microscope was used to acquire the image.

30



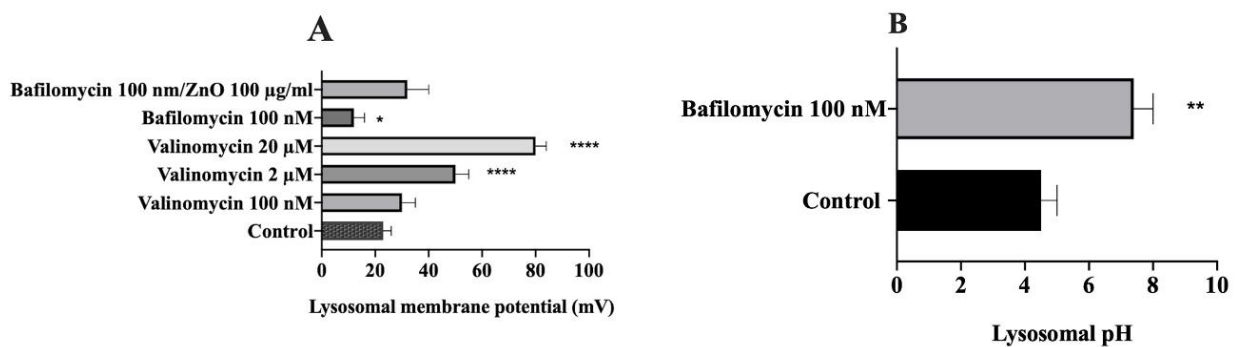
31

32 **Figure S4.** Lack of pH dependency of the DiBAC4(3) quantum yield. A) Spectra of
 33 fluorescent intensity of DiBAC4(3) in PBS at different pHs. Fluorimetric
 34 analysis was performed in quartz cuvettes using a Spectramax M4 fluorescence
 35 spectrometer. B) Fluorescent intensity of DiBAC4(3) in PBS at different pHs
 36 (emission 518 nm). Data are presented as means \pm SE of triplicate
 37 measurements.



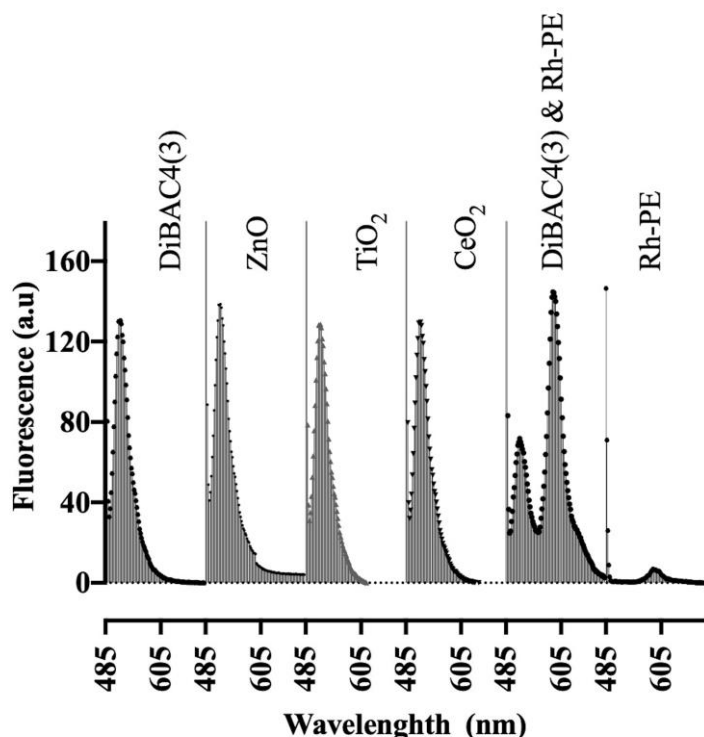
38

39 **Figure S5.** Fluorescence intensity of DiBAC4(3) at different concentrations. A)
 40 Fluorescence emission traces of a titration of DiBAC4(3). Fluorimetric analysis
 41 was performed in quartz cuvettes using a Spectramax M4 fluorescence
 42 spectrometer. B) The calibration curve was calculated based on the peak
 43 fluorescent intensity of each concentration at 518 nm.



44

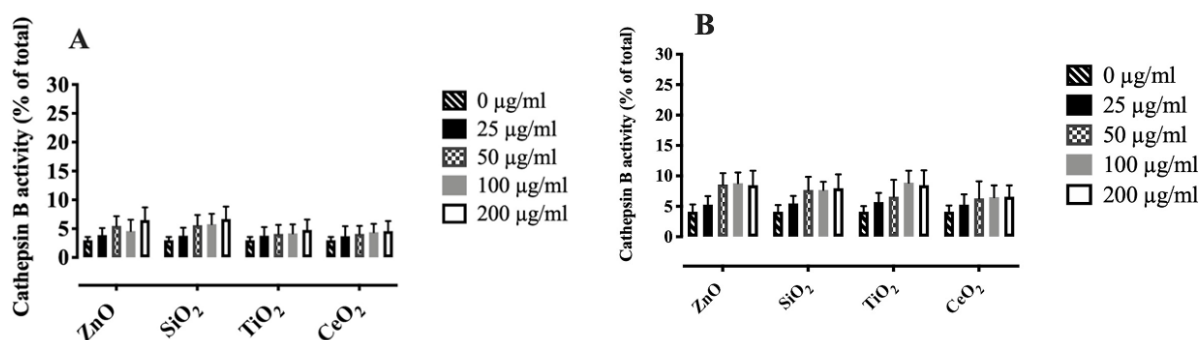
45 **Figure S6. The importance of K⁺ and H⁺ in maintaining lysosomal membrane**
 46 **potential.** A) Lysosomal membrane potential was manipulated with Valinomycin or
 47 Bafilomycin A1. AM were incubated with Valinomycin or Bafilomycin A1 for 1 hr at
 48 37°C and lysosomal membrane potential was determined as discussed in the Methods.
 49 B) The effect of Bafilomycin on lysosomal pH. AM were incubated with Bafilomycin
 50 A1 for 1 hr at 37°C and lysosomal pH was determined with LysoSensor Yellow/Green
 51 as discussed in the Methods. Data are presented as means \pm SE of triplicate
 52 measurements. *, **, and **** indicates significant effect (P \leq 0.05, P \leq 0.01, and
 53 P \leq 0.0001, respectively).



54

55

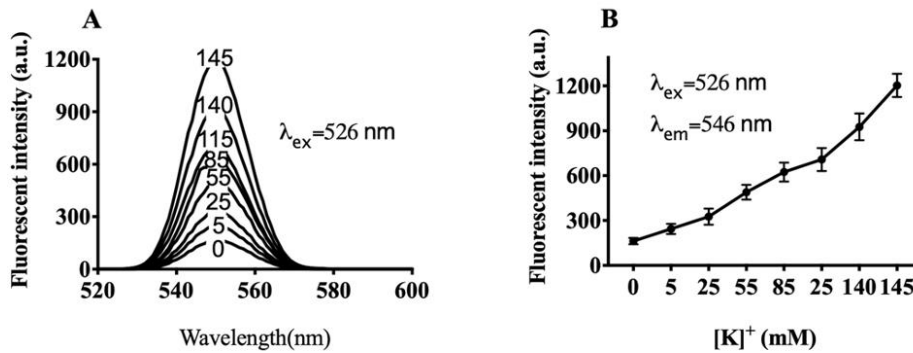
56 **Figure S7.** NP do not interfere with DiBAC4(3) or the fluorescent signal generated.
 57 Small unilamellar vesicles composed of L- α -phosphatidylcholine (Egg-PC) with or
 58 without individual NP were prepared by the extrusion method. The emission fluorescent
 59 spectra of liposome with and without NP was measured with spectrophotometry as
 60 discussed in the Methods. Liposome containing DiBAC4(3) and its quencher, L- α -
 61 phosphatidylethanolamine-N-lissamine rhodamine B sulfonyl (Rh-PE) was used as a
 62 control for fluorescent intensity reduction of DiBAC4(3). The area under curve of the
 63 spectra (liposome with and without NP) was calculated using Prism software.



64

65 **Figure S8. Lysosomal membrane permeabilization of AM treated with NP or SiO₂.**
 66 AM were incubated with individual particles for 1 and 2 hr at 37°C and cathepsin B
 67 release was determined as discussed in the Methods. Results from the release of
 68 cathepsin B into the cytoplasm was used as an indicator of LMP and was evaluated

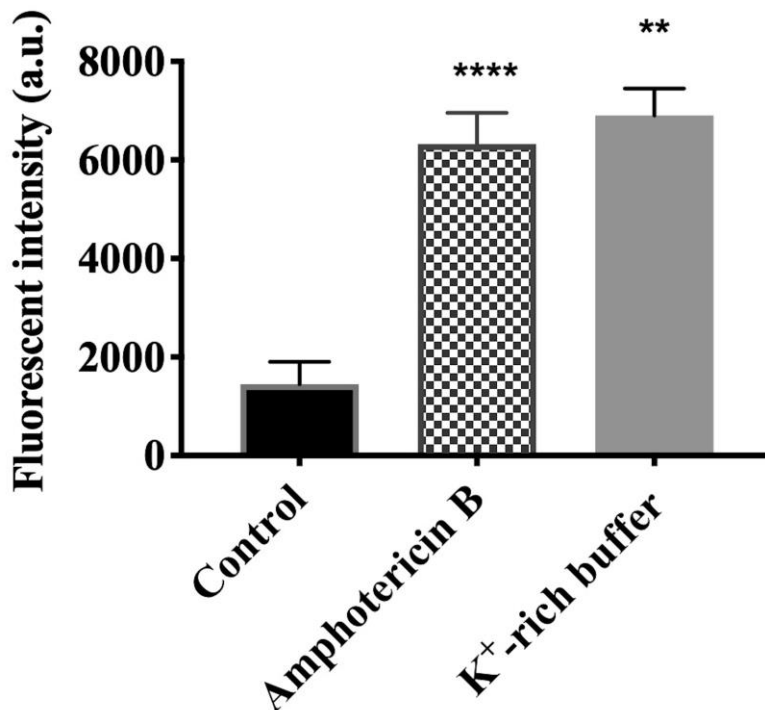
69 using digitonin as described in Methods. LMP assay after incubation of particles with
 70 AM for A) 1 hr, B) 2 hr. Data are presented as means \pm SE of triplicate measurements.



71

72

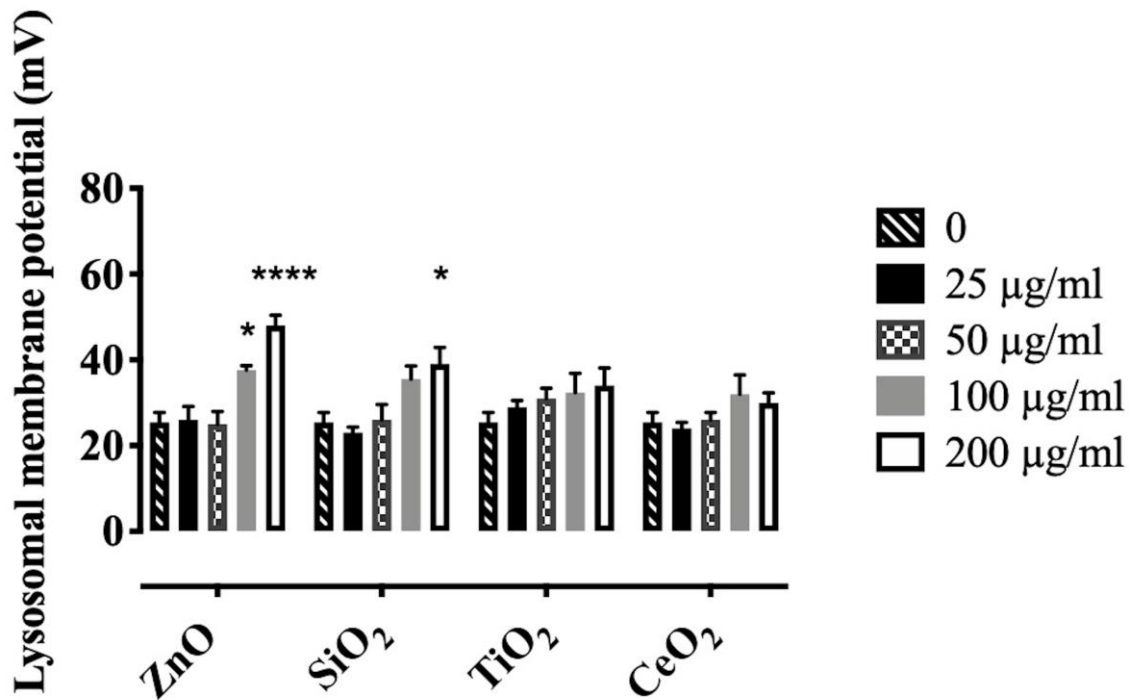
73 **Figure S9. Spectrofluorimetric characterization of APG-2, a K⁺ indicator.** A)
 74 Emission spectra recorded in the presence of different K⁺ in intracellular-like
 75 solutions as described in Methods. Fluorimetric analyses were performed in
 76 quartz cuvettes using a Spectramax M4 fluorescence spectrometer. B)
 77 Fluorescence emission plotted as a function of K⁺ showing a positive
 78 relationship of K⁺ indicator fluorescence with increasing K⁺.



79

80 **Figure S10.** Amphotericin B-, or K⁺-rich buffer-induced plasma membrane
 81 depolarization in alveolar macrophages (AM). Plasma membrane potential was

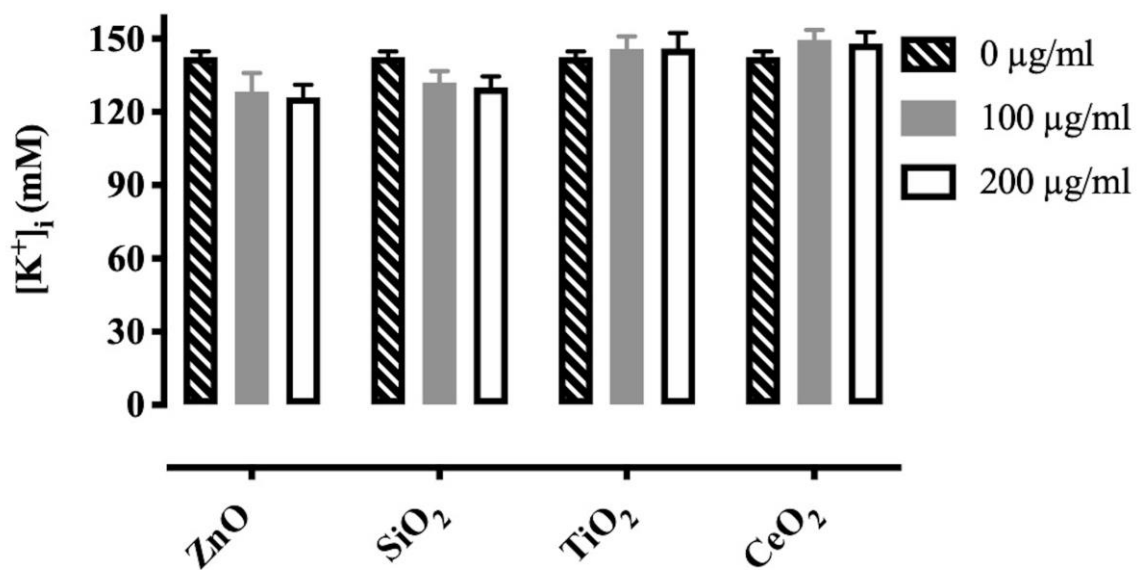
82 measured as described in Methods. Data are presented as means \pm SE of
83 triplicate measurements. **** Indicates significant effect ($P \leq 0.0001$).



84

85 **Figure S11. Particle-induced hyperpolarization is the result of lysosomal K⁺ influx**
86 **rather than cytosolic K⁺ efflux.** AM suspended in K⁺-rich buffer were incubated with
87 individual particles for 1 hr at 37°C. Control cells were incubated in the same
88 experimental condition without particle. Lysosomal membrane potential changes
89 (hyperpolarization) were calculated as described in Methods. A Zeiss LSM 880
90 confocal microscope and ZEN imaging software (ZEISS) as well as ImageJ were used
91 for our studies. The fluorescent intensity of at least 100 cells was measured and
92 analyzed using ZEN imaging software (ZEISS) and ImageJ. Statistical analysis was
93 performed using Prism software. Data are presented as means \pm SE of triplicate
94 measurements. *, **, and **** indicate significant effects ($P \leq 0.05$, $P \leq 0.01$ and
95 $P \leq 0.0001$, respectively).

96



97

98

99 **Figure S12.** Cytosolic K⁺ decrease due to particles is the result of lysosomal K⁺ influx
 100 rather than cytosolic K⁺ efflux. Cytosolic K⁺ was measured using acetoxymethyl ester of
 101 APG-2 and a SpectraMax M4 spectrofluorometer as described in Methods. AM
 102 suspended in K⁺-rich buffer were incubated with NP or SiO₂ for 1 hr at 37°C. Data are
 103 presented as means ± SE of triplicate measurements.

104 1.

105